AEM Accepted Manuscript Posted Online 20 February 2015
Appl. Environ. Microbiol. doi:10.1128/AEM.00067-15

C:N ratio drives soil actinobacterial cellobiohydrolase gene diversity

Alexandre B. de Menezes[1#], Miranda T. Prendergast-Miller[2], Pabhon Poonpatana[3], Mark Farrell[2], Andrew Bissett[1], Lynne M. Macdonald[2], Peter Toscas[4], Alan E. Richardson[1] and Peter H. Thrall[1]

[1]CSIRO Agriculture Flagship, Crace, Canberra, ACT 2911, Australia
[2]CSIRO Agriculture Flagship, Waite Campus, Glen Osmond, SA 5068, Australia
[3]Queensland University of Technology, Brisbane, QLD 4000 Australia
[4]CSIRO Digital Productivity and Services Flagship, Clayton South, VIC 3169, Australia

#Address correspondence to: A. B. de Menezes, email: ademenez@gmail.com
CSIRO Agriculture Flagship, GPO Box 1600, Canberra ACT, Australia
Telephone: +61 (2) 62465041, Fax +61 (2) 62464950

Running title: Actinobacterial cellulase gene ecology in soil

Abstract

Cellulose accounts for approximately half of photosynthesis fixed carbon, however the ecology of its degradation in soil is still relatively poorly understood. The role of actinobacteria in cellulose degradation has not been extensively investigated, despite their abundance in soil and known cellulose degradation capability. Here, the diversity and abundance of the actinobacterial glycoside hydrolase family 48 (cellobiohydrolase) gene was determined in soils from three paired pasture-woodland sites using T-RFLP and clone libraries with gene-specific primers. For comparison, the diversity and abundance of general bacteria and fungi were also assessed. Phylogenetic analysis of the nucleotide sequences of 80 clones revealed significant new diversity of actinobacterial GH48 genes, and analysis of translated protein sequences showed that these are likely to represent functional cellobiohydrolases. Soil C:N ratio was the primary environmental driver of GH48 community composition across sites and land uses, demonstrating the importance of substrate quality in their ecology. Furthermore, mid infrared (MIR) spectrometry-predicted humic organic carbon was distinctly more important to GH48 diversity than to total bacterial and fungal diversity. This suggests a link between actinobacterial GH48 community and soil organic carbon dynamics and highlights the potential importance of actinobacteria in the terrestrial carbon cycle.

1. Introduction

Cellulases are responsible for the degradation of cellulose, an insoluble, recalcitrant substrate which comprises approximately half of the biologically fixed CO_2 on earth (1). Cellulases are classified as glycosyl hydrolases (GH) together with other enzymes that target the glycosidic bonds in oligo- and polysaccharides, and are grouped into families that reflect their protein folding structure (2). Metagenomic studies have characterized various cellulose-rich environments, such as the bovine rumen (3-6), rabbit caecum (7), ant fungus gardens (8), compost (9, 10), earthworm casts (11), termite gut (12) and forest soil (13, 14). These studies have revealed a rich new GH gene diversity not thus far observed in cultured microorganisms. However, little is known about the role of GH genes in natural environments and the enzymes they encode.

Glycoside hydrolases are a large and complex group of enzymes, with some GH families showing multiple substrate specificity (15). Horizontal gene transfer has also been documented for many GH families (15-21). The presence of multiple substrate specificity within the same GH family has precluded the design of molecular tools for in-depth investigation of their environmental role. Importantly, all 13 functionally characterised bacterial glycoside hydrolase family 48 (GH48) enzymes have been shown to target cellulose and, in most bacteria that carry the GH48 gene, it is present as a single genomic copy (19). Only in insects have the characterised GH48 enzymes been shown not to target cellulose; in these organisms GH48 enzymes are chitinases.

In conventional systems for cellulase classification, GH48 enzymes mostly function as cellobiohydrolases, also known as exoglucanases (22). This class of cellulases are known to hydrolyse the ends of the cellulose chain and to act processively, producing glucose or cellobiose as end products (15). Although their specific activity is low, GH48 cellobiohydrolases are important components of the multi-enzyme cellulolytic systems they are part of, acting in synergy with other cellulases in order to achieve efficient depolymerisation of cellulose. The deletion of GH48 genes from bacterial genomes has been shown to significantly impair cellulolytic activity (23-25). GH48 cellobiohydrolases are prevalent amongst Gram-positive cellulose degraders, but are also found in anaerobic fungi (order Neocallimastigales), a small number of Gram-negative bacteria and in certain insects (19, 21, 26, 27).

Evolutionary analysis of GH48 sequences obtained from bacterial, fungal and insect genomes suggests that GH48 genes evolved in the common ancestor of phyla Actinobacteria, Firmicutes and the Chloroflexi, and their occurrence outside these phyla is due to horizontal gene transfer (19). Sukharnikov et al. (19) also identified a conserved omega loop in all functionally characterised bacterial GH48 proteins which is absent in insect GH48 proteins, and used the presence of this loop and conserved residues in the catalytic region of GH48 gene to predict that all known bacterial and fungal GH48 enzymes target cellulose. In addition to cellulose, the GH48 enzymes of some *Clostridium* species are known to also hydrolyse xylan, mannan and β-glucan in addition to cellulose (28-30). Studies have investigated the diversity and abundance of GH48 genes from anaerobic Gram-positive bacteria such as *Clostridium* spp. in thermophilic composts, sulphate-reducing bioreactors and wastewater sediments (22, 31, 32), and one study has investigated actinobacterial GH48 gene diversity in decomposing straw (33).

Members of the Actinobacteria phylum are abundant in soils and are thought to have an important role in organic matter turn-over, breakdown of recalcitrant molecules such as cellulose (34, 35), and polycyclic aromatic hydrocarbons (36). Cultivation-based studies have demonstrated the ability of many actinobacteria to grow on cellulose (37-39), whilst the properties of actinobacterial cellulolytic enzymes have been characterised for two model cellulose-degrading strains, *Thermobifida fusca* and *Cellulomonas fimi* (40, 41). Furthermore, analysis of the available actinobacterial genomes has shown the presence of functional GH genes which are similar to characterised cellulase genes in *T. fusca* and *C. fimi* (42, 43). Further analysis of their cellulolytic ability indicated that most actinobacteria that contain functional cellulase genes are able to degrade cellulose, whereas the absence of detectable activity in laboratory assays may be a result of the use of modified cellulose substrates and artificial growth media not optimal for cellulase production and activity (43). It is important to note that efficient cellulose degradation can only occur through the concerted action of several enzymes (i.e. endoglucanases, cellobiohydrolases and β-glucosidases) (15), and therefore it is not possible to estimate cellulose degradation rates through the detection and quantification of a single cellulose-degradation gene. However the development of tools for determination of the abundance and diversity of one of the most substrate-specific cellulose degradation genes (the GH48 gene) from actinobacteria will aid in elucidating the ecology and the role of these organisms in terrestrial carbon cycling.

In this study we investigated the ecology of saprotrophic actinobacteria in soil by developing standard and quantitative PCR primers targeting the catalytic region of the actinobacterial GH48 gene. We aimed to determine whether the GH48 gene community would correlate more strongly to soil carbon quantity and quality than the overall bacterial and fungal communities. Cloning and sequencing was used to determine the phylogeny of actinobacterial GH48 genes amplified from soils. We investigated the presence of the catalytic base residue and residues involved in substrate recognition and cellulose chain accessibility in order to assess whether these represented functional GH48 genes likely to be involved in cellulose degradation. Quantitative PCR was used to provide an estimate of the abundance of these genes in the soils analysed. Using terminal restriction fragment length polymorphism (T-RFLP) we assessed the diversity of soil actinobacterial GH48 genes from three paired pasture-woodland sites. Specifically we contrasted actinobacterial GH48 ecology in two systems where plant litter is likely to be chemically and structurally different (44, 45). Furthermore, soil variables were quantified and used to develop multivariate correlation models of actinobacterial GH48, general bacterial 16S rRNA and fungal ITS genes.

2. Material and Methods

2.1. Field sites

Sampling was conducted at three paired sites, each comprising adjacent 1 ha pasture and woodland plots. The sites were Talmo (34.936976°S, 148.625293°E), Glenrock (34.858413°S, 148.56724°E) and Bogo (34.813746°S, 148.704558°E) and are located on farms near the locality of Bookham, NSW, Australia (46). The woodland sites were dominated by *Eucalyptus* spp. [(*Eucalyptus melliodora* A. Cunn. Ex Schaur (yellow box) and *E. albens* Benth. (white box)]; Talmo woodland plot had the highest tree densities with an infrequent population of *Acacia dealbata* and *Acacia implexa* and small isolated patches of native Australian grasses, such as *Themeda triandra* Forssk. and *Poa sieberiana* Spreng. The pasture plots were improved with *Trifolium subterraneum* (subterranean clover) and show a mixture of annual and perennial native and introduced grasses, including *Phalaris aquatica*. The pasture plots were routinely grazed with sheep and received regular inputs of phosphorus fertiliser (approximately 10 kg P ha^{-1} yr^{-1}), with Talmo and Glenrock having higher level of overall soil fertility and stocking rates. For further site description details see de Menezes et al. (46) and Supplementary Material.

A total of 240 samples were taken across the six plots. Soils cores (0-10 cm deep, 5 cm diameter) were kept cold (4°C) until processed. The soils were sieved (5 mm), homogenised and separated into aliquots: a) frozen in liquid nitrogen (for DNA analyses); b) kept at 4°C (quantification of soil nutrients and moisture); c) air dried (soil pH, mid infrared (MIR) spectrometry and C and N analyses). Soil properties [pH, soil moisture, dissolved organic carbon (DOC), dissolved organic nitrogen (DON), ammonium (NH_4^+-N), nitrate (NO_3^--N), free amino acids (FAA-N), microbial biomass C (MBC), microbial biomass N (MBN), loss on ignition (LOI), total, inorganic and organic P, total C and N and particulate-, humus- and resistant-organic carbon (POC, HOC and ROC)] were determined as described in de Menezes et al. (46). There is a high correlation between the MIR predictive algorithms used to estimate HOC and total organic carbon (TOC), which indicates that these two organic carbon fractions are predicted based on the same MIR spectral features (47). Therefore the interpretation of HOC as humic organic carbon should be taken with caution. For more details regarding the organic carbon fraction determination by MIR, see Supplementary Material.

2.2. GH48 primer design

2.2.1. Standard GH48 PCR primers

All 39 unique available actinobacterial GH48 sequences were obtained from the CAZy web portal (http://www.cazy.org/) (48) and aligned in MAFFT using the accuracy oriented global pair (G-INS-i) method (49). Alignments were visualised in Geneious v. 5.6.6 (Biomatters, New Zealand), and conserved regions were identified that partially covered the GH48 catalytic domain [1923 bp long in *T. bifida* (24)]. Primers were designed using the primer design tool in Geneious. Due to the difficulties in designing one primer pair covering all actinobacterial GH48 gene diversity, two primer pairs were developed, GH48_F1 (5'-

RRCATBTACGGBATGCACTGGCT-3’) and GH48_R1 (5’-VCCGCCCCABGMGTARTACC-3’) as well as GH48_F1_cell (5’-AYGTCGACAACRTSTACGGMTWCG-3’) and GH48_R1_cell (5’ CCGCCCCASGCSWWRTACC-3’), and both were used for cloning and sequencing and T-RFLP. In-silico primer specificity was analysed using MFEprimer-2.0 (50), which revealed that the combination of the two primer pairs provided good coverage of known actinobacterial GH48 gene diversity (see the Results section 3.1.). Further details of GH48 gene primer design are in supplementary Supplementary Material Tables S1 and S2.

2.2.2. Quantitative-PCR primer design

GH48 qPCR primers (qPCR_GH48_F8: 5’-GCCADGHTBGGCGACTACCT-3’ and qPCR_GH48_R5: 5’- CGCCCCABGMSWWGTACCA-3’) were designed as above, based on sequences obtained from the CAZy database. Further details of GH48 gene primer design are in Supplementary methods and Supplementary Tables S1 and S2.

2.3. DNA extraction

The MoBio PowerSoil® kit (Carlsbad, CA) was used to extract DNA from 0.25 g of soil, according to the manufacturer’s instructions except for the use of a Qiagen TissueLizer (Venlo, Netherlands) shaker for 2 minutes at full speed after the introduction of buffer C1. DNA concentrations were normalised across all samples as reported by de Menezes et al. (46).

2.4. Cloning

The 40 DNA samples from each of the 6 plots (total of 240 samples from the 3 paired pasture-woodland sites) were pooled and amplified with both GH48 PCR primer pairs (GH48_F1-GH48_R1 and GH48_F1_cell-GH48_R1_cell) to give 12 amplifications. Each of the 12 amplicon fragments were excised and purified from 1% agarose gels using QIAquick® spin Miniprep kits (Qiagen, Düsseldorf, Germany). Amplicons were then cloned from each of the 12 amplicon mixtures separately using the Promega pGEM®-T Easy vector system (Promega, Madison, USA). Resulting plasmids containing inserts of the correct length were extracted using Perfectprep® plasmid isolation kits (Eppendorf, Hamburg, Germany) and the clones sequenced by Macrogen (Seoul, South Korea) using M13 primers. Sequences were analysed in Geneious and poor quality sequences removed from the dataset. A total of 80 high quality GH48 sequences were obtained from the 12 cloning reactions which were then used for phylogenetic analyses, with a total 39 sequences from woodlands and 41 for pastures, and 9 to 16 sequences per individual pasture or woodland plot.

The actinobacterial GH48 gene sequences generated in this study were submitted to GenBank (accession numbers KM891594-KM891673).

2.5. Phylogenetic analysis of actinobacterial GH48 sequences

Available GH48 sequences (excluding duplicates) from cultured actinobacteria strains, as well as a selection of sequences from the Firmicutes (*Bacillus* spp., *Paenibacillus* spp., *Clostridium* spp.), Proteobacteria (*Hahella chejuensis* and *Myxobacter* sp.), Chloroflexi (*Herpetosiphon aurantiacus*), anaerobic fungi (*Piromyces* spp. and *Neocallimastix* spp.) and Insecta (*Leptinotarsa decemliuneata*) were aligned in MAFFT (49) using the G-INS-i model and default parameters for DNA alignment. The alignment was visualised and manually optimised in Geneious and exported after removal of the primer regions. After alignment, nucleotide sequences were translated into protein sequences; any sequence that did not translate into a GH48 through its entire length was removed from the original nucleotide sequence alignment prior to the construction of phylogenetic trees.

Maximum Likelihood phylogenetic trees were produced by exporting the alignment to PhyML online (http://atgc.lirmm.fr/phyml/) (51) and RaxML (http://phylobench.vital-it.ch/raxml-bb/) (52). PhyML was run using the HKY85 substitution model and the Shimoidara-Hasegawa (SH)-like aLRT branch support method and 100 bootstraps. RaxML was run with 100 bootstraps and the CAT model of heterogeneity (52). The tree topologies generated with PhyML and RaxML were compared to determine the consistency of tree branching patterns. The resulting RaxML phylogenetic trees were uploaded in iTol (http://itol.embl.de) (53) for visualisation of the phylogeny and metadata (see Supplementary Material Fig. S2 for the PhyML tree).

2.6. Analysis of residues of functional significance

The GH48 sequence region targeted in this study corresponds to the region in the *T. fusca* gene that contains the catalytic base D225 (aspartic acid) essential for cellulose hydrolysis (54), as well as 12 other residues conserved in bacterial and fungal GH48 cellobiohydrolases with functional significance in substrate recognition (hydrogen bonding and hydrophobic stacking interactions) and enzyme thermal stability (calcium coordination) (19, 55, 56). In addition, the region targeted also includes two aromatic residues (phenylalanine 195 and tyrosine 213) in the entrance of the *T. fusca* GH48 active site tunnel (in which the cellulose chain slides in and where hydrolysis take place) which play a role in facilitating access of the cellulose chains to the active site and promote enzyme processivity (57). In order to determine if the GH48 sequences obtained here also had these residues, the 80 aligned GH48 sequences produced from our clone libraries were translated to protein sequences and compared with the protein sequence of the model organism *T. fusca*.

2.7. qPCR cycling conditions

GH48, bacterial 16S rRNA and fungal ITS gene abundances were quantified from each of the 240 individual soil samples in triplicate reactions using the SsoAdvanced™ SYBR® green Supermix (Bio-Rad, Hercules, CA) using the C1000 Thermal cycler (Bio-Rad, Hercules, CA), to which 400 nM primers, 2 µl DNA (diluted 1 in 10) and H_2O were added to 10 µl. qPCR cycling conditions were as follows: for the GH48 gene, 95°C for 1 min. (1 cycle), 95°C for 5s, 57°C for 20s (39 cycles); 16S rRNA gene rRNA [primers Eub338 (58) and Eub518 (59)], 95°C for 1 min. (one cycle), 95°C for 15s and 56°C for 20s (39 cycles); ITS1 gene [primers ITS1F (60) and 5.8s (61)], 95°C for 1 minute (one cycle), 95°C for 5s and 53°C for 20s and extension at 72°C (39 cycles). A melt curve from 65°C to 95°C was added at the end of all amplification cycles. Standards were run in triplicates in each qPCR plate with 10-fold dilution series from 10^8 to 100 copies μl^{-1}. GH48 standards were purified PCR products from a local soil actinobacterial isolate; for bacteria and fungi the PCR products from *Pseudomonas fluorescens* strain 5.2 16S rRNA or the ITS gene from *Fusarium oxysporum vasinfectum* were used. Amplification efficiencies were > 90% and R^2 was > 0.99 for all GH48, bacterial 16S rRNA and fungal ITS gene calibration curves.

2.8. T-RFLP analysis

2.8.1. GH48 gene

For T-RFLP analysis of the 240 individual soil samples, multiplex PCR was performed using both primer pairs designed for the actinobacterial GH48 gene (GH48_F1-GH48_R1 and GH48_F1_cell-GH48_R1_cell). The GH48_F1 and GH48_F1_cell primers were labelled with 6-Carboxyfluorescein and 5-Hexachlorofluorescein at the 5'end, respectively. The PCR reactions contained 2 ng DNA, forward and reverse primers (200 nM each), MyTaq™ DNA polymerase (0.25 µl) (Bioline, Alexandria, Australia), dNTP (250 µM each) and 1x of the supplied buffer. A touchdown-PCR protocol was used for GH48 gene amplification as follows: 95°C for 2 minutes, followed by 2 cycles of 30s each at 95°C, 65°C and 72 °C; 2 cycles of 30s each at 95°C, 62°C and 72°C; 3 cycles of 30s at 95°C and 59°C and 40s at 72°C; 4 cycles of 30s at 95°C and 56°C and 45s at 72°C; 5 cycles of 30s at 95°C and 53°C and 50s at 72°C; 30 cycles of 30s at 95°C, 45s at 50°C, and 100s at 72°C; lastly 1 cycle at 72°C for 10 minutes. The amplified PCR products were cleaned with Agencourt® AMPure® beads (Beckman Coulter, Lane Cove, Australia) and quantified using a Quant-iT™ Picogreen® dsDNA quantification kit (Life Technologies™, Mulgrave, Australia) according to the manufacturer's instructions. 25 ng of PCR product was added to a reaction mixture containing water, reaction buffer and 20 units of the *Alu*I and *Mbo*II restriction enzymes (New England Biolabs); the double-digestion was carried out overnight at 37°C. For the purification of PCR products, digests were precipitated by incubation with 150 µl of cold 75% isopropanol (v/v) (Sigma-Aldrich, Sydney, Australia) for 30 minutes followed by centrifugation at 4000 rpm for 45 minutes. Purified PCR products were added to a reaction containing Hi-Di™ formamide (9.7 µl) and GeneScan™ 600 LIZ size standard (0.3 µl) (Applied Biosystems, Mulgrave, Australia). After denaturation (94°C for 3 minutes) fragment lengths were determined by electrophoresis using an AB3031xl Genetic Analyzer (Applied Biosystems, Mulgrave, Australia). GENEMAPPER® (Applied Biosystems, Mulgrave, Australia) was used to provide restriction fragment profiles and these were filtered using the method of Abdo et al. (62) to remove spurious baseline peaks (minimum height of 20 fluorescence units; peaks smaller than 2 times the standard deviation calculated over all peaks were removed). The resulting GH48 gene sizing data was binned using Interactive Binner (63) in R (64) with a sliding window approach and the following parameters: minimum and maximum peak sizes of 40 and 520 bp repectively; minimum relative fluoresence units of 0.099, window size of 2.5 bp and a shift size of 0.25 bp.

2.8.2. Bacteria and fungal T-RFLP analysis

Briefly, DNA from bacteria was amplified using primers 27f (58) and 519r (65) and the fungal ITS region using primers ITS1f (66) and ITS4 (60). For both fungi and bacteria the forward primer was 6-FAM labelled at the 5' end. The amplicon mixtures of both groups were digested with *Alu*I (New England Biolabs), and the resulting digests were processed and analysed as described in de Menezes et al. (46).

2.9. Statistical analysis

2.9.1. Data analysis

Multivariate statistical analysis were carried out in PRIMER 6 and PERMANOVA+ (Primer-E Ltd., Plymouth, UK) (67). GH48, bacterial 16S rRNA and fungal ITS gene community ribotype relative abundance data obtained by T-RFLP were square-root transformed and a Bray-Curtis dissimilarity matrix calculated. Soil variables were fourth-root transformed (except pH) and standardised, and a Euclidean distance matrix calculated. In order to visualise differences in GH48, bacterial 16S rRNA and fungal ITS gene composition across sites and land uses, ordination by principal coordinate (PCO) analysis was carried out. The vector overlay function in PRIMER was used to visualise the soil variables that correlated with the first two PCO axes. Only variables that had a vector length > 0.4 were included for visualisation in the PCO plot. The vector length is calculated based on the correlations between the soil variable in question and the first two PCO axes and indicate the strength and sign of the relationship between the soil variable and the PCO axes (68).

PERMANOVA analysis (performed with a non-nested fixed factors design, type III partial sums of squares and 9999 permutations under a reduced model) was used to determine differences in GH48 community composition between pasture and woodlands, between sites and the interaction between site and land use. For PERMANOVA there were 2 factors: site [3 levels (Talmo, Glenrock and Bogo)], and land use [2 levels (woodland and pasture)]. Multivariate dispersion index analysis (MVDISP) was used to quantify β-diversity (community composition heterogeneity) amongst samples within each land use as well as among samples in each pasture and woodland plot, whilst significance of differences in β-diversity between land uses and sites was determined using a test of homogeneity of dispersion (PERMDISP), using 9999 permutations.

SIMPER analysis (analysis of contribution of variables to similarity) was used to determine the variability of soil properties (67) across land uses and sites and was calculated using the Euclidean distance matrix of the 4^{th} root transformed (except pH) and standardised soil variable dataset.

2.9.2. DistLM

The relationships between GH48 gene community composition and soil parameters were determined using non-parametric multivariate multiple regressions (DistLM) from the PERMANOVA+ add-on in PRIMER-E package. DistLM was conducted using the stepwise selection procedure with the adjusted R^2 selection criterion and 9999 permutations. Soil variables that were correlated with each other ($r^2 > 0.9$) were removed from the dataset except the predicted organic carbon fractions (HOC, ROC and POC), as a specific goal was to investigate the importance of carbon fractions of different quality. Total C was removed as it was correlated with predicted HOC and ROC, and N was removed as it was correlated with predicted POC in the woodlands. Total P was also removed as it was correlated with organic P.

3. Results

3.1. In-silico PCR and qPCR primer specificity analysis

A thermodynamic in-silico analysis of PCR amplification was performed to determine whether the primers developed here showed good specificity and coverage of known actinobacterial GH48 genes. The two standard GH48 PCR primer pairs developed showed differences in their coverage of actinobacterial GH48 diversity (Supplementary Material Tables S1 and S2). The GH48_F1 - GH48_R1 primer pair were found to be capable of amplifying GH48 genes from every actinobacterial genus present in the Cazy database except *Cellulomonas* and *Cellvibrio*, however 10 out of 16 GH48 sequences from *Streptomyces* strains were not predicted to be amplified by the GH48_F1 - GH48_R1 primer pair (see Supplementary Material Table S1). Primer pair GH48_F1_cell and GH48_R1_cell was predicted to amplify all available GH48 gene sequences from the *Cellulomonas, Xylanimonas* and *Jonesia* genera as well as *Cellvibrio gilvus*. In addition GH48_F1_cell and GH48_R1_cell primers were predicted to amplify seven *Streptomyces* strains not expected to be amplified by GH48_F1-GH48_R1 primers. However GH48_F1_cell and GH48_R1_cell were not predicted to amplify GH48 sequences from several actinobacterial genera such as *Nocardiopsis*, *Salinispora*, *Catenulispora*, *Streptosporangium* and *Thermobifida.* Overall coverage of actinobacterial GH48 diversity was therefore lower, but complementary to that of GH48_F1-GH48_R1 primers. Both primer pairs missed three *Streptomyces* GH48 sequences present in the databases, and in combination the two primer pairs are predicted to amplify 36 out of 39 actinobacterial GH48 gene sequences (Supplementary Material Table S1). The primers GH48_F1-GH48_R1 were predicted to amplify *Hahella chejuensis*, a member of the Gammaproteobacteria phylum that acquired this gene by horizontal gene transfer (19). No non-GH48 genes are predicted to be amplified by the GH48_F1-GH48_R1 or GH48_F1_cell-GH48_R1_cell primer pairs (Supplementary Material Table S1). Therefore, in-silico analysis demonstrated that in combination the two standard PCR-primer pairs developed here provided good specificity and coverage of known actinobacterial GH48 genes.

The GH48 qPCR primers developed here covered a narrower range of actinobacterial GH48 diversity compared to the standard GH48 primers and were not predicted to amplify 15 out of 39 GH48 gene sequences from cultured actinobacterial strains (Supplementary Material Table S1). As with the standard PCR primers, no non-GH48 genes are predicted to be amplified by the qPCR_GH48_F8 and qPCR_GH48_R5 primer pair (Supplementary Material Table S1). Therefore, the qPCR primer pair developed here underestimates the total abundance of the actinobacterial GH48 gene, and is only used to estimate a minimum abundance of actinobacterial GH48 genes in the soils studied.

3.2. Phylogenetic analysis of GH48 clones

Cloning and sequencing of the PCR products obtained with both GH48_F1-GH48_R1 and GH48_F1_cell-GH48_R1_cell primer pairs was conducted for further evaluation of primer specificity, and to determine the phylogenetic relationships of the amplified soil GH48 genes to those of cultured actinobacteria. A total of 87 high quality sequences were obtained, of which three were removed due to the presence of stop codons in the sequence. A further four sequences were removed as translation did not result in a GH48 protein sequence for the entire region covered. One sequence was removed as no close database matches could be identified by BLASTn. Of the remaining 80 clones, 77 were unique sequences.

Comparison of phylogenetic trees generated by PhyML and RaxML revealed consistent branching patterns. GH48 sequences from cultured actinobacterial strains formed a separate cluster to those from other cultured bacteria and eukaryotes; however, this cluster had low bootstrap support. All but two (PhyML) or four (RaxML) of the 80 soil clones from this study clustered with the actinobacteria (Fig. 1 and Supplementary Material Fig. S2), and BLASTn analysis of these divergent clones showed that their top hits remained as GH48 genes from cultured actinobacteria. However, the possibility that a small proportion of amplified sequences were not derived from the actinobacteria cannot be ruled out.

Neither PhyML or RaxML phylogenetic analysis showed any pronounced clustering of sequences arising from either land use, or from any of the sites studied. There was no clustering of sequences arising from the use of either primer pair, and therefore the diversity recovered with both standard-PCR GH48 primer sets designed in this study were similar at the sequencing depth investigated here.

Closer inspection of the phylogenetic tree shown in Fig. 1 and Supplementary Material Fig. S2 revealed that some of the sequences obtained clustered with known actinobacterial GH48 genes, whilst the majority of clones formed new clusters without any cultured representative. All streptomycete sequences grouped in one cluster in both the PhyML and RaxML trees, and this cluster, which had high bootstrap support in the RaxML tree (> 0.8) included two soil clone sequences. A second cluster with high bootstrap support in the trees generated with both methods included *Catenulispora acidiphila* and 18 soil clones. RaxML indicated that two clones clustered with high bootstrap support with *Actinoplanes* spp., and one soil clone clustered with *Verrucosispora maris*. PhyML also showed the presence of these clusters but with lower bootstrap support. Both the RaxML and PhyML phylogenetic tree revealed that most soil clones were located in clusters, which did not contain any GH48 sequences from cultured strains. The largest of these clusters had 22 soil clones, while other clusters containing only soil clones had 16, seven and three clones. There were four soil clones that clustered adjacent to a *Salinispora-Micromonospora-Verrucosispora* cluster. There were two soil clones that clustered with low bootstrap support with *Hahella chejuensis* from the Gammaproteobacteria phylum. The phylogenetic tree obtained by RaxML, but not PhyML, showed that two other soil clones were located outside of the actinobacteria cluster, although clearly separate from the Firmicute and eukaryote clusters.

3.3. Analysis of residues of functional significance

In order to evaluate whether the amplified GH48 genes were likely to be functional cellobiohydrolase genes, the presence of conserved residues with known roles in substrate recognition, accessibility and hydrolysis was determined. All of the clones obtained in this study showed the presence of the catalytic base, a conserved aspartic acid residue in the same position as *T. fusca* D225 (Fig. 1). Analysis of 12 conserved residues with functional roles in bacterial and fungal GH48 cellobiohydrolases (Supplementary Material Table S3) show that all 8 conserved residues involved in hydrogen bonding were present in > 89% of the sequences obtained in this study, and six of these were present in > 98% of the GH48 clones. One residue involved with calcium coordination was present in 71% of the GH48 clones obtained. Two further conserved residues involved with calcium coordination and hydrophobic stacking interactions were present in 47-57% of the clones, however these residues were absent from the GH48 protein sequence of the model cellulose-degrading actinobacteria *T. fusca*. Fig. 1 shows the presence or absence of aromatic residues which have a demonstrated role in providing access to cellulose chains in the *T. fusca* GH48 enzyme. All but six soil clones showed the presence of either or both aromatic residues of functional significance (phenylalanine 195 and tyrosine 213). Inspection of the GH48 sequences from cultured strains revealed that all actinobacterial sequences had either one or both conserved aromatic residues, whilst the presence of these residues in the Firmicutes GH48 sequences was more variable, and none of the fungal sequences showed their presence.

3.4. GH48 diversity in woodlands and pastures

GH48 gene diversity across sites and land uses was determined by T-RFLP and their community composition was analysed against measured soil properties to provide an understanding of which environmental variables drive GH48 gene ecology. Principal coordinate analysis of the GH48 gene diversity (Fig. 2A) revealed a broad separation of samples by land use although some overlap of samples from woodland and pasture was observed, particularly between Talmo woodland and Glenrock pasture. Separation of samples by site was less clear, and samples from Glenrock and Bogo overlapped substantially within each land use. PCO analysis also showed a greater spread of woodland samples compared to those from the pastures. The main PCO axis explained 26.2% of the total variation and the vector overlay function suggests that C:N ratio (positive correlation with main PCO axis) and soil moisture (negative correlation with main PCO axis) were the main soil variables influencing GH48 community composition in the sites investigated. The soil C:N ratio vector correlated mostly with shifts in woodland GH community composition whilst moisture mostly correlated with changes in the GH48 composition of pasture samples, particularly those of Talmo pasture. Glenrock and Bogo pastures as well as Talmo woodland samples were spread along along the C:N ratio – moisture axis in the PCO plot.

In order to contrast the ecology of the actinobacterial GH48 gene with that of the overall soil microbial community, the diversity and community composition of bacterial 16S rRNA and fungal ITS genes were also analysed. PCO analysis of bacterial 16S rRNA gene diversity (Fig. 2B) showed that pasture and woodland samples were broadly separated along the second PCO axis, which explained 9% of the total variation in community composition. The C:N ratio and soil moisture vectors were positively and negatively correlated with the second PCO axis, respectively, and were the two main soil variables explaining shifts in bacterial community composition. However, PCO analysis showed that shifts in pasture bacterial community composition also correlated (> 0.4) with the vectors for MBC, MBN, pH, NO_3^--N, predicted POC, total, inorganic and organic P and total N. PCO analysis of fungal community diversity (Fig. 2C) showed that pasture and woodland samples were separated along the main PCO axis, which explained 11.7% of the variation in community composition. The C:N ratio and soil moisture vectors were positively and negatively correlated with the main PCO axis, respectively, and the soil moisture vector also correlated negatively with the second PCO axis. The fungal pasture communities from each site were separated along the second PCO axis. Shifts in fungal community composition from Glenrock pasture samples correlated with the NH_4^+-N vector, shifts in fungal community composition from Bogo pasture samples correlated with the NO_3^--N, inorganic P, TDN, total N and total P vectors whilst shifts in fungal community composition from Talmo pasture correlated with the soil moisture, pH, MBC, MBN, predicted POC and organic P vectors. Shifts in fungal community composition from all woodland sites correlated with the C:N vector.

PERMANOVA analysis was conducted to determine if the differences in community composition between land uses and sites were statistically significant. Table 1 shows that GH48 community composition was significantly different between land uses and between sites ($p < 0.001$), and PERMANOVA Pseudo-F suggests that GH48 community composition was more different between land uses than among sites, however an interaction effect between site and land use suggests that this difference was not uniform across sites. Pairwise PERMANOVA comparisons showed that differences in GH48 community composition between land uses at each site were greater than differences between sites at each land use except when comparing Talmo and Bogo samples.

MVDISP analysis was performed to determine whether the GH48 gene showed similar patterns of community composition heterogeneity across sites and land uses as the bacterial and fungal communities. In addition, variability in soil properties was also analysed using SIMPER. Table 2 shows that the GH48 gene composition was more heterogeneous in the woodlands compared to the pastures. PERMDISP indicated that this difference was significant ($p < 0.001$). The MVDISP and PERMDISP analysis of individual woodland and pasture plots revealed that whilst Talmo and Bogo pastures had low heterogeneity levels, Glenrock pasture heterogeneity was of a similar level to those of the woodland plots (Table 2). PERMDISP showed that differences in community heterogeneity were not significant between the individual woodland plots and between woodland plots and Glenrock pasture, but

Talmo and Bogo pastures had significantly lower heterogeneity levels compared to all other plots (Table 2).

Bacterial heterogeneity levels were similar between the combined woodland and pasture pots, whilst when analysing each individual plot, Talmo and Bogo Woodland had the highest heterogeneity levels. Fungal communities were more heterogeneous in the woodlands, and the higher heterogeneity of the woodland fungal communities was observed both when comparing all woodlands to all pastures as well as when analysing each individual plot (Table 2). The variability of soil parameters (Table 2), followed a similar pattern to that seen for GH48 gene and fungal community heterogeneity, and was higher at the woodland plots.

3.5. Factors driving GH48, general bacterial and fungal community composition

Multivariate correlation models were built using DistLM to provide a quantitative description of the contributions of each measured soil property to the observed patterns of variability in community composition for the GH48, 16S rRNA and fungal ITS genes (Table 3). When analysing the combined land use dataset, a similar set of soil variables made the highest contribution to the variability of the three groups investigated, in particular C:N ratio and soil moisture. Notable differences between groups include a greater importance of organic P and MBC in the bacterial model; organic P in particular was the second most important factor in explaining bacterial community composition variability, whereas this variable had little impact in the GH48 functional community and fungal models. Predicted HOC explained a higher proportion of GH48 community composition variability than for the other two groups. Predicted ROC and POC, DON, NH_4^+-N, MBC, clay and inorg. P were included in all three models, but generally made smaller contributions to explaining community composition variability. A greater proportion of community composition variability was explained in the bacterial model (R^2=0.35), than for GH48 (R^2=0.23) or fungal communities (R^2=0.25).

In woodlands samples alone, pH explained a similar (for the GH48 gene and fungal communities) or higher (for bacteria) amount of variability than C:N ratio compared to the combined land use models. Predicted HOC and soil moisture were relatively important in the GH48 gene model but did not contribute to a significant extent or at all in explaining variability in the bacterial and fungal DistLM models. The bacterial model explained more community composition variability (R^2=0.36), followed by the GH48 (R^2=0.16) and fungal (R^2=0.13) community models.

Soil moisture explained more community composition variability in pasture compared to the woodland DistLM models. While inorganic P was the variable that explained the most variability of the bacterial community and the second most important variable in the fungal model, it was not part of the GH48 community model. Predicted HOC was the second variable that most explained variability of the GH48 community model, whereas in the bacterial and fungal models predicted HOC was comparatively less important. Clay, pH and predicted POC were included in the models of the three groups. As with the combined land use model, the bacterial model had highest amount of explained variability (R^2 = 0.47), followed by the fungal (R^2 = 0.29) and GH48 models (R^2 = 0.21).

3.6. Total and relative abundance of GH48, 16S rRNA and fungal ITS genes

The abundance of the GH48 gene was determined and compared to that of the bacterial 16S rRNA and fungal ITS genes in order to estimate the relative importance of actinobacterial saprotrophs to the overall microbial community (Fig. 3). Results show that whilst at Talmo GH48 abundance was similar in both land uses, at the other sites the abundance in pastures were 5-13 fold greater than in the woodlands in Glenrock and Bogo respectively. Bacterial 16S rRNA abundance was greater in the pastures compared to the woodlands at Talmo (1.79 fold) and Glenrock (1.9 fold) but not in Bogo (1.04 fold). Fungal ITS total abundance was greater in pastures compared to woodlands at Talmo (2.7 fold) and Bogo (2.2 fold) but not at Glenrock (0.34 fold).

4. Discussion

4.1. GH48 PCR Primer specificity

In silico analysis of standard PCR primers developed here indicated that the two primer sets are broadly complementary in their actinobacterial GH48 diversity coverage, and in combination cover almost all the actinobacterial GH48 diversity from cultured strains available in GenBank (Supplementary Material Tables S1 and S2). The high level of specificity of the GH48 primers to actinobacterial GH48 genes indicated by in-silico analysis is corroborated by the fact that only 1 out of 87 high quality clone sequences represented a non-GH48 sequence. One non-actinobacterial GH48 sequence (*Hahella chejuensis*) was a predicted target of primers GH48_F1-GH48_R1. This species is a member of the Gammaproteobacteria phylum and acquired the GH48 gene by horizontal gene transfer (19). Phylogenetic analysis of the GH48 clone sequences did indeed indicate that 4 clones may be of non-actinobacterial origin. This represents a relatively low level of non-specificity (< 5%), and in any case the gene amplified was a GH48 gene, indicating that these primers are highly specific to the targeted gene ecological function they were designed for.

The in-silico specificity analysis of the GH48 qPCR primers developed here showed that this primer pair was unlikely to amplify any template other than actinobacterial GH48 genes; however the qPCR primers did not cover all actinobacterial GH48 gene diversity from cultured actinobacterial strains and therefore provided an underestimation of actual actinobacterial GH48 gene abundances (Supplementary Material Tables S1 and S2).

As with any PCR-based approach, the standard- and quantitative-PCR primers developed here will not amplify GH48 genes that do not share sequence similarity in the PCR primer target sites. However, application of these primers for the determination of diversity and abundance patterns across a large number of samples, in concert with the determination of soil properties, allows a better understanding of the ecological role of saprotrophic actinobacteria in soil ecology and carbon cycling.

4.2. Diversity of actinobacterial GH48 genes in soils

Phylogenetic analysis of soil GH48 sequences revealed significant new diversity not covered in gene databases (Fig. 1 and Supplementary Material Fig. S2). The majority of sequences were located in clusters without any cultured representative, although a large number of sequences clustered with high bootstrap support with *Catenulispora acidiphila*, and a smaller number of soil clones clustered with *Streptomyces* spp., *Actinoplanes* spp. and *Verrucosispora maris*. GH48 gene sequence data is only available for 17 actinobacterial genera, and this low coverage of GH48 gene diversity from cultured actinobacteria precludes a better understanding of the phylogenetic identity of the soil clones obtained here. No obvious clustering of sequences derived from woodlands or pastures, or from a specific site, was observed.

All the soil clones obtained showed the presence of the catalytic base aspartic acid 225 as determined for *T. fusca* (Fig. 1), which plays the essential role of activating the catalytic water molecule that allows hydrolysis of the β-1,4 glycosidic bonds in cellulose (54).

Additionally, conserved residues present in the targeted region which are involved with substrate recognition were conserved in the majority of the clones obtained here (Supplementary Material Table S3). The three conserved residues whose presence was more variable in the clones obtained were also absent in the GH48 protein sequence of model cellulolytic organism *T. fusca*, or were not involved in substrate recognition, which would suggest that their presence is not essential for cellulose degradation activity in actinobacteria. Furthermore all but 6 soil clones showed the presence of either or both aromatic amino acids (F195 and Y213) in the entrance of the GH48 catalytic tunnel (Fig. 1) (57). The absence of the F195 and Y213 residues would not necessarily indicate lack of cellulolytic function; indeed the sequences from *Xylanimonas cellulolytica, Actinosynnema mirum* and *Nocardiopsis dassonvillei,* which are known to possess the ability to degrade cellulose (43) lack the Y213 aromatic residue. The presence of the catalytic base, conserved residues involved in substrate recognition and key aromatic amino acid residues in the majority of the GH48 sequences obtained in this study is an indication that these clones represent functional cellobiohydrolases.

4.3. Actinobacterial GH48 gene community diversity across land uses

PCO analysis showed that C:N ratios and soil moisture were the two main drivers of GH48 community composition across all sites and land uses, opposing most Talmo pasture samples (high in soil moisture) to Talmo, Bogo and Glenrock woodlands (high C:N ratio) (Fig. 2A). The C:N ratio are thought to influence litter C availability and high C:N ratio has a negative effect on extracellular hydrolytic enzymes during litter decomposition (69, 70). It is not surprising therefore that C:N ratio was one of the vectors with strongest correlations to the main PCO axis, and was more important than the levels of organic soil carbon fractions themselves.

As with the GH48 gene PCO analysis, C:N ratio and soil moisture were also the two main drivers of the overall bacterial and fungal community composition (Figs. 2B and 2C); however other soil properties were comparatively more important in explaining community composition shifts of these broader groups than those of the GH48 gene community composition. As the primers developed here target a more specific microbial functional group (i.e. actinobacterial saprotrophs), the lower importance of other soil variables may simply reflect the narrower physiological range of the GH48 gene community.

Whilst clustering of samples based on land use and site can be discerned, some overlap between samples from different sites and land uses was observed, particularly between Talmo woodland, Glenrock woodland and Glenrock pasture samples. PERMANOVA analysis was able to demonstrate that actinobacterial GH48 community composition was significantly different between all sites and between land uses, whilst pairwise comparisons confirmed that GH48 community composition was significantly different between pasture and woodlands at every site and between sites in both land uses (Table 1).

β-diversity estimated using multivariate dispersion analysis showed that the actinobacterial GH48 and fungal communities were more heterogeneous in the woodlands, whilst the β-diversity of the bacterial community was more similar between the two land uses (Table 2). The heterogeneity of the GH48 and fungal communities broadly tracked the variability of soil properties which is also greater in the woodlands. These results suggest that the community assembly processes of GH48 and fungal communities are more strongly influenced by the measured soil properties than is the case for the bacterial community. The similarity in heterogeneity patterns between the GH48 and fungal communities is interesting given that a significant proportion of soil fungi have a similar, but not identical, ecological niche in soil (i.e. soil saprotrophs capable of degrading plant-cell wall polysaccharides).

In Glenrock pasture the GH48 community was as heterogeneous as those of the woodland plots. It is not possible to determine the reason for the high levels of heterogeneity at Glenrock pasture, but this site had the highest and most variable overall C:N ratio of all pastures (46). Given the importance of C:N ratios in structuring GH48 community composition, it is possible that the ecology of the actinobacterial GH48 community at Glenrock pasture was more similar to the woodlands than to the other pastures investigated here.

4.4. Soil carbon influence on GH48, bacterial and fungal community composition

Predicted HOC was found to be consistently more important to the variability of the GH48 community compared to the general bacterial and fungal communities based on the DistLM analysis (Table 3). These results agree with the saprotrophic lifestyle expected of GH48 gene-carrying actinobacteria (34, 71), which represent a more ecologically defined microbial group compared to the overall bacterial and fungal communities. Whilst other bacterial and fungal groups are also likely to have a saprotrophic role in these soils, the general fungal and bacterial communities analysed here represent broad metabolic groups with diverse ecological roles, and their association with soil organic fractions are therefore less obvious. Our data indicates therefore that we were successful in targeting actinobacteria with saprotrophic lifestyle that are likely involved with organic C dynamics in these soils.

The precise nature of the predicted HOC fraction measured here is currently unknown; further studies are necessary to determine whether cellulose is a component of this fraction and whether saprotrophic actinobacteria are able to scavenge cellulose from a matrix of less bioavailable compounds such as peptidoglycan, lignin, and lipids (72, 73). The association of saprotrophic actinobacteria with soil organic carbon found here agrees with the results of Baldrian et al. (74), which showed increased actinobacterial abundance in the deeper humic horizon of forest soils.

HOC was the most abundant fraction of predicted soil organic carbon in the sites studied, representing approximately 50% of the combined carbon from all MIR resolved C-fractions (46) and this is also the case in a range of soils from Australia (47). The data obtained here therefore highlight the potential importance of soil actinobacteria in the turnover of this more recalcitrant C pool and thus their impact on the carbon cycle.

4.5. Other factors influencing community composition

Soil moisture in the woodlands was noticeably more important for the GH48 community model than for the general bacterial and fungal models (Table 3). The woodland soils at the time of sampling were relatively dry, and considerably drier than the pastures (46), where moisture was one of the most important variables for the three microbial groups investigated. It is possible that the greater importance of moisture in the woodland GH48 compared to the bacterial and fungal DistLM models was a result of their community composition, as tracked by their DNA, more accurately reflected the active community, whilst a large proportion of the community composition tracked by the general 16S rRNA and ITS genes may have been inactive or senescent, capturing growth that occurred during past periods of higher moisture. This is corroborated by a study showing that actinobacteria were more dominant in the RNA rather than DNA fractions in spruce forest soils, particularly in the deeper humic horizon (74). Inorganic P was the first and second most important soil variable explaining variability in the bacterial and fungal models in the pastures, respectively; the impact of P fertilisation on soil bacterial and fungal community composition has been previously documented (75). By contrast, the best GH48 community pasture DistLM model did not include inorganic P. The soil P levels determined in this study represent an approximation of soluble, plant-available organic and inorganic P (76, 77) and the application of P fertilizer was the major anthropologically-driven difference between each of the paired woodland and pasture sites. The low importance of inorganic P in actinobacterial GH48 models suggest that these organisms obtain most of their P requirements directly from decomposing organic matter (which unlike soluble orthophosphate is not immediately plant-available), even when more easily available inorganic P is present.

DistLM analysis further revealed that for the GH48, bacterial and fungal communities, pH and particularly C:N ratio played a smaller role in structuring composition in the pastures compared to the woodlands, whilst moisture was considerably more important than in the woodlands. C:N ratios in the pasture soils were lower (52 - 65%) and less variable than in the woodlands (46), which probably accounts for its lower impact on community composition in the pastures. Moisture and pH were more correlated with each other in the pastures ($r=0.67$) than in the woodlands ($r=0.30$); their co-correlation most likely lowered the additional variability explained by pH, once the variability explained by moisture was included in the DistLM model.

4.6. GH48 abundance in relation to bacteria and fungi.

The quantification of GH48 genes showed a higher abundance of GH48 in Glenrock and Bogo pastures, whereas bacterial and fungal abundances in these pastures were similar to or lower than those in the woodlands (Fig. 3). As the qPCR primers developed here do not cover all of the cultured GH48 gene diversity it is not possible to determine whether the higher abundances in Glenrock and Bogo pastures are caused by higher total gene abundances or by differences in the taxonomical composition of the GH48 community between those pastures and the other plots. However, it is interesting that Bogo pasture had the lowest overall C:N ratio and the highest overall GH48 abundance; likewise Bogo woodlands had the lowest C:N ratio and the highest GH48 abundance amongst woodlands (46). This pattern would agree with studies showing that higher C:N ratios are negatively correlated to extracellular hydrolytic enzyme activity during litter decomposition (69).

5. Conclusions

This study is to our knowledge the first soil-based, landscape-scale investigation of the diversity of a cellobiohydrolase gene in relation to different land uses and soil properties. Our data revealed significant new diversity of actinobacterial GH48 genes and that C:N ratio and moisture are primary factors driving GH48 community composition in the soils studied. Given the ubiquity and abundance of actinobacteria in soils their role in soil carbon cycling clearly merits further attention. Finally, we have laid the groundwork necessary for further studies to investigate the diversity of actinobacterial GH48 genes in soil. Future studies focusing on in-situ expression of this cellobiohydrolase gene should provide a better understanding of the ecological role of these organisms in soil C cycling, and their interactions with other soil saprotrophs.

6. Acknowledgements

We are particularly grateful to Tony Armour (Glenrock), Chris Shannon (Talmo), and Malcolm Peake (Bogo) for their enthusiastic support of this research, and their willingness to allow us access to their properties. Shamsul Hoque (CPI) provided excellent technical support in the lab and field.

7. References

1. **Ljungdahl LG, Eriksson KE.** 1985. Ecology of microbial cellulose degradation. Adv Microb Ecol **8:**237-299.
2. **Henrissat B.** 1998. Glycosidase families. Biochem Soc T **26:**153-156.
3. **Qi M, Wang P, O'Toole N, Barboza PS, Ungerfeld E, Leigh MB, Selinger LB, Butler G, Tsang A, McAllister TA, Forster RJ.** 2011. Snapshot of the eukaryotic gene expression in muskoxen rumen - a metatranscriptomic approach. Plos One **6**.
4. **Brulc JM, Antonopoulos DA, Miller MEB, Wilson MK, Yannarell AC, Dinsdale EA, Edwards RE, Frank ED, Emerson JB, Wacklin P, Coutinho PM, Henrissat B, Nelson KE, White BA.** 2009. Gene-centric metagenomics of the fiber-adherent bovine rumen microbiome reveals forage specific glycoside hydrolases. P Natl Acad Sci USA **106:**1948-1953.
5. **Duan CJ, Xian L, Zhao GC, Feng Y, Pang H, Bai XL, Tang JL, Ma QS, Feng JX.** 2009. Isolation and partial characterization of novel genes encoding acidic cellulases from metagenomes of buffalo rumens. J Appl Microbiol **107:**245-256.
6. **Ferrer M, Golyshina OV, Chernikova TN, Khachane AN, Reyes-Duarte D, Dos Santos V, Strompl C, Elborough K, Jarvis G, Neef A, Yakimov MM, Timmis KN,**

Golyshin PN. 2005. Novel hydrolase diversity retrieved from a metagenome library of bovine rumen microflora. Environ Microbiol **7:**1996-2010.

7. **Feng Y, Duan CJ, Pang H, Mo XC, Wu CF, Yu Y, Hu YL, Wei J, Tang JL, Feng JX.** 2007. Cloning and identification of novel cellulase genes from uncultured microorganisms in rabbit cecum and characterization of the expressed cellulases. Appl Microbiol Biot **75:**319-328.

8. **Suen G, Scott JJ, Aylward FO, Adams SM, Tringe SG, Pinto-Tomás AA, Foster CE, Pauly M, Weimer PJ, Barry KW, Goodwin LA, Bouffard P, Li L, Osterberger J, Harkins TT, Slater SC, Donohue TJ, Currie CR.** 2010. An insect herbivore microbiome with high plant biomass-degrading capacity. Plos Genet **6**.

9. **Pang H, Zhang P, Duan C-J, Mo X-C, Tang J-L, Feng J-X.** 2009. Identification of cellulase genes from the metagenomes of compost soils and functional characterization of one novel endoglucanase. Curr Microbiol **58:**404-408.

10. **Allgaier M, Reddy A, Park JI, Ivanova N, D'Haeseleer P, Lowry S, Sapra R, Hazen TC, Simmons BA, VanderGheynst JS, Hugenholtz P.** 2010. Targeted discovery of glycoside hydrolases from a switchgrass-adapted compost community. Plos One **5**.

11. **Beloqui A, Nechitaylo TY, López-Cortés N, Ghazi A, Guazzaroni M-E, Polaina J, Strittmatter AW, Reva O, Waliczek A, Yakimov MM, Golyshina OV, Ferrer M, Golyshin PN.** 2010. Diversity of glycosyl hydrolases from cellulose-depleting communities enriched from casts of two earthworm species. Appl Environ Microb **76:**5934-5946.

12. **Warnecke F, Luginbühl P, Ivanova N, Ghassemian M, Richardson TH, Stege JT, Cayouette M, McHardy AC, Djordjevic G, Aboushadi N, Sorek R, Tringe SG,**

Podar M, Martin HG, Kunin V, Dalevi D, Madejska J, Kirton E, Platt D, Szeto E, Salamov A, Barry K, Mikhailova N, Kyrpides NC, Matson EG, Ottesen EA, Zhang XN, Hernández M, Murillo C, Acosta LG, Rigoutsos I, Tamayo G, Green BD, Chang C, Rubin EM, Mathur EJ, Robertson DE, Hugenholtz P, Leadbetter JR. 2007. Metagenomic and functional analysis of hindgut microbiota of a wood-feeding higher termite. Nature **450:**560-U517.

13. **Uroz S, Buee M, Murat C, Frey-Klett P, Martin F.** 2010. Pyrosequencing reveals a contrasted bacterial diversity between oak rhizosphere and surrounding soil. Environ Microbiol Rep **2:**281-288.

14. **Takasaki K, Miura T, Kanno M, Tamaki H, Hanada S, Kamagata Y, Kimura N.** 2013. Discovery of glycoside hydrolase enzymes in an avicel adapted forest soil fungal community by a metatranscriptomic approach. Plos One **8**.

15. **Lynd LR, Weimer PJ, van Zyl WH, Pretorius IS.** 2002. Microbial cellulose utilization: fundamentals and biotechnology. Microbiol Mol Biol R **66:**506-577.

16. **Gilbert HJ, Hazlewood GP, Laurie JI, Orpin CG, Xue GP.** 1992. Homologous catalytic domains in a rumen fungal xylanase - evidence for gene duplication and prokaryotic origin. Mol Microbiol **6:**2065-2072.

17. **Garcia-Vallvé S, Palau J, Romeu A.** 1999. Horizontal gene transfer in glycosyl hydrolases inferred from codon usage in *Escherichia coli* and *Bacillus subtilis*. Mol Biol Evol **16:**1125-1134.

18. **Garcia-Vallvé S, Romeu A, Palau J.** 2000. Horizontal gene transfer of glycosyl hydrolases of the rumen fungi. Mol Biol Evol **17:**352-361.

19. **Sukharnikov LO, Alahuhta M, Brunecky R, Upadhyay A, Himmel ME, Lunin VV, Zhulin IB.** 2012. Sequence, structure, and evolution of cellulases in glycoside hydrolase family 48. J Biol Chem **287:**41068-41077.

20. **Palomares-Rius JE, Hirooka Y, Tsai IJ, Masuya H, Hino A, Kanzaki N, Jones JT, Kikuchi T.** 2014. Distribution and evolution of glycoside hydrolase family 45 cellulases in nematodes and fungi. BMC Evol Biol **14**.

21. **Quillet L, Barray S, Labedan B, Petit F, Guespin-Michel J.** 1995. The gene encoding the β-1,4-endoglucanase (celA) from *Myxococcus xanthus* - evidence for independent acquisition by horizontal transfer of binding and catalytic domains from actinomycetes. Gene **158:**23-29.

22. **Izquierdo JA, Sizova MV, Lynd LR.** 2010. Diversity of bacteria and glycosyl hydrolase family 48 genes in cellulolytic consortia enriched from thermophilic biocompost. Appl Environ Microb **76:**3545-3553.

23. **Olson DG, Tripathi SA, Giannone RJ, Lo J, Caiazza NC, Hogsett DA, Hettich RL, Guss AM, Dubrovsky G, Lynd LR.** 2010. Deletion of the Cel48S cellulase from *Clostridium thermocellum*. P Natl Acad Sci USA **107:**17727-17732.

24. **Irwin DC, Zhang S, Wilson DB.** 2000. Cloning, expression and characterization of a Family 48 exocellulase, Cel48A, from *Thermobifida fusca*. Eur J Biochem **267:**4988-4997.

25. **Devillard E, Goodheart DB, Karnati SKR, Bayer EA, Lamed R, Miron J, Nelson KE, Morrison M.** 2004. *Ruminococcus albus* 8 mutants defective in cellulose degradation are deficient in two processive endocellulases, Cel48A and Cel9B, both of which possess a novel modular architecture. J Bacteriol **186:**136-145.

26. **Steenbakkers PJM, Freelove A, van Cranenbroek B, Sweegers BMC, Harhangi HR, Vogels GD, Hazlewood GP, Gilbert HJ, den Camp H.** 2002. The major component of the cellulosomes of anaerobic fungi from the genus *Piromyces* is a family 48 glycoside hydrolase. DNA Sequence **13:**313-320.

27. **Ramírez-Ramírez N, Romero-García ER, Calderón VC, Avitia CI, Téllez-Valencia A, Pedraza-Reyes M.** 2008. Expression, characterization and synergistic interactions of *Myxobacter* sp AL-1 Cel9 and Cel48 glycosyl hydrolases. Int J Mol Sci **9:**247-257.

28. **Shen H, Gilkes NR, Kilburn DG, Miller RC, Warren RAJ.** 1995. Cellobiohydrolase B, a second exo-cellobiohydrolase from the cellulolytic bacterium *Cellulomonas fimi*. Biochem J **311:**67-74.

29. **Liu CC, Doi RH.** 1998. Properties of exgS, a gene for a major subunit of the *Clostridiun cellulovorans* cellulosome. Gene **211:**39-47.

30. **Berger E, Zhang D, Zverlov VV, Schwarz WH.** 2007. Two noncellulosomal cellulases of *Clostridium thermocellum*, Cel9I and Cel48Y, hydrolyse crystalline cellulose synergistically. FEMS Microbiol Lett **268:**194-201.

31. **Pereyra LP, Hiibel SR, Riquelme MVP, Reardon KF, Pruden A.** 2010. Detection and quantification of functional genes of cellulose-degrading, fermentative, and sulfate-reducing bacteria and methanogenic archaea. Appl Environ Microb **76:**2192-2202.

32. **Yang CY, Wang W, Du MF, Li CF, Ma CQ, Xu P.** 2013. Pulp mill wastewater sediment reveals novel methanogenic and cellulolytic populations. Water Res **47:**683-692.

33. **Zhang X, Zhong Y, Yang S, Zhang W, Xu M, Ma A, Zhuang G, Chen G, Liu W.** 2014. Diversity and dynamics of the microbial community on decomposing wheat straw during mushroom compost production. Bioresource Technol **170:**183-195.

34. **Goodfellow M, Williams ST.** 1983. Ecology of Actinomycetes. Annu Rev Microbiol **37:**189-216.

35. **McCarthy AJ.** 1987. Lignocellulose-degrading actinomycetes. FEMS Microbiol Rev **46:**145-163.

36. **de Menezes A, Clipson N, Doyle E.** 2012. Comparative metatranscriptomics reveals widespread community responses during phenanthrene degradation in soil. Environ Microbiol **14:**2577-2588.

37. **Phelan MB, Crawford DL, Pometto AL.** 1979. Isolation of lignocellulose-decomposing actinomycetes and degradation of specifically labelled ^{14}C-labelled lignocelluloses by six selected *Streptomycete* strains. Can J Microbiol **25:**1270-1276.

38. **Ulrich A, Klimke G, Wirth S.** 2008. Diversity and activity of cellulose-decomposing bacteria, isolated from a sandy and a loamy soil after long-term manure application. Microb Ecol **55:**512-522.

39. **de Menezes AB, Lockhart RJ, Cox MJ, Allison HE, McCarthy AJ.** 2008. Cellulose degradation by micromonosporas recovered from freshwater lakes and classification of these actinomycetes by DNA Gyrase B gene sequencing. Appl Environ Microb **74:**7080-7084.

40. **Rabinovich ML, Melnik MS, Bolobova AV.** 2002. Microbial cellulases (Review). Appl Biochem Microbiol **38:**305-321.

41. **Teeri TT.** 1997. Crystalline cellulose degradation: New insight into the function of cellobiohydrolases. Trends Biotechnol **15:**160-167.

42. **Koeck DE, Pechtl A, Zverlov VV, Schwarz WH.** 2014. Genomics of cellulolytic bacteria. Curr Opin Biotech **29:**171-183.

43. **Anderson I, Abt B, Lykidis A, Klenk H-P, Kyrpides N, Ivanova N.** 2012. Genomics of aerobic cellulose utilization systems in *Actinobacteria*. Plos One **7**.

44. **Kögel-Knabner I.** 2002. The macromolecular organic composition of plant and microbial residues as inputs to soil organic matter. Soil Biol Biochem **34:**139-162.

45. **Austin AT, Ballaré CL.** 2010. Dual role of lignin in plant litter decomposition in terrestrial ecosystems. P Natl Acad Sci USA **107:**4618-4622.

46. **de Menezes AB, Prendergast-Miller MT, Richardson AE, Toscas P, Farrell M, Macdonald LM, Baker G, Wark T, Thrall PH**. Network analysis reveals that bacteria and fungi form modules that correlate independently with soil parameters. Environ Microbiol (In Press, doi:10.1111/1462-2920.12559).

47. **Baldock JA, Hawke B, Sanderman J, Macdonald LM.** 2013. Predicting contents of carbon and its component fractions in Australian soils from diffuse reflectance mid-infrared spectra. Soil Res **51:**577-583.

48. **Lombard V, Ramulu HG, Drula E, Coutinho PM, Henrissat B.** 2014. The carbohydrate-active enzymes database (CAZy) in 2013. Nucleic Acids Res **42:**D490-D495.

49. **Katoh K, Kuma K, Toh H, Miyata T.** 2005. MAFFT version 5: improvement in accuracy of multiple sequence alignment. Nucleic Acids Res **33:**511-518.

50. **Qu W, Zhou Y, Zhang Y, Lu Y, Wang X, Zhao D, Yang Y, Zhang C.** 2012. MFEprimer-2.0: a fast thermodynamics-based program for checking PCR primer specificity. Nucleic Acids Res **40:**W205-W208.

51. **Guindon S, Dufayard J-F, Lefort V, Anisimova M, Hordijk W, Gascuel O.** 2010. New algorithms and methods to estimate maximum-likelihood phylogenies: assessing the performance of PhyML 3.0. Systematic Biol **59:**307-321.

52. **Stamatakis A, Hoover P, Rougemont J.** 2008. A rapid bootstrap algorithm for the RAxML web servers. Systematic Biol **57:**758-771.

53. **Letunic I, Bork P.** 2007. Interactive Tree Of Life (iTOL): an online tool for phylogenetic tree display and annotation. Bioinformatics **23:**127-128.

54. **Kostylev M, Wilson DB.** 2011. Determination of the catalytic base in family 48 glycosyl hydrolases. Appl Environ Microb **77:**6274-6276.

55. **Parsiegla G, Reverbel C, Tardif C, Driguez H, Haser R.** 2008. Structures of mutants of cellulase Ce148F of *Clostridium cellulolyticum* in complex with long hemithiocellooligosaccharides give rise to a new view of the substrate pathway during processive action. J Mol Biol **375:**499-510.

56. **Guimarães BG, Souchon H, Lytle BL, Wu JHD, Alzari PM.** 2002. The crystal structure and catalytic mechanism of cellobiohydrolase CelS, the major enzymatic component of the *Clostridium thermocellum* cellulosome. J Mol Biol **320:**587-596.

57. **Kostylev M, Alahuhta M, Chen M, Brunecky R, Himmel ME, Lunin VV, Brady J, Wilson DB.** 2014. Cel48A from *Thermobifida fusca*: structure and site directed mutagenesis of key residues. Biotechnol Bioeng **111:**664-673.

58. **Lane DJ.** 1991. 16S/23S rRNA sequencing, p. 115-175. *In* Stackebrandt E, Goodfellow, M (ed.), Nucleic acid techniques in bacterial systematics. John Wiley & Sons, Chichester, UK.

59. **Muyzer G, Dewaal EC, Uitterlinden AG.** 1993. Profiling of complex microbial populations by denaturing gradient gel electrophoresis analysis of polymerase chain

reaction-amplified genes coding for 16s ribosomal RNA. Appl Environ Microb **59:**695-700.

60. **White TJ, T. Burns, S.Lee, J. Taylor** 1990. Amplification and direct sequencing of fungal ribosomal RNA genes for phylogenetics, p. 315-322. *In* Innis M, D.H. Gelfand, J.J. Sninsky, T.J. White (ed.), PCR protocols. Academic Press, San Diego.

61. **Vilgalys R, Hester M.** 1990. Rapid genetic identification and mapping of enzymatically amplified ribosomal DNA from several *Cryptococcus* species. J Bacteriol **172:**4238-4246.

62. **Abdo Z, Schüette UME, Bent SJ, Williams CJ, Forney LJ, Joyce P.** 2006. Statistical methods for characterizing diversity of microbial communities by analysis of terminal restriction fragment length polymorphisms of 16S rRNA genes. Environ Microbiol **8:**929-938.

63. **Ramette A.** 2009. Quantitative community fingerprinting methods for estimating the abundance of operational taxonomic units in natural microbial communities. Appl Environ Microb **75:**2495-2505.

64. **R Core Development Team.** 2014. R: A Language and Environment for Statistical Computing. R Foundation for Statistical Computing, Viena, Austria.

65. **Lane DJ, Pace B, Olsen GJ, Stahl DA, Sogin ML, Pace NR.** 1985. Rapid determination of 16S ribosomal RNA sequences for phylogenetic analyses. P Natl Acad Sci USA **82:**6955-6959.

66. **Gardes M, Bruns TD.** 1993. ITS primers with enhanced specificity for basidiomycetes - application to the identification of mycorrhizae and rusts. Mol Ecol **2:**113-118.

67. **Clarke K, Gorley R.** 2006. PRIMER v6: User Manual/Tutorial, Plymouth, UK.

68. **Anderson M, Gorley R, Clarke K.** 2008. PERMANOVA+ for PRIMER, user manual, Plymouth, UK.

69. **Leitner S, Wanek W, Wild B, Haemmerle I, Kohl L, Keiblinger KM, Zechmeister-Boltenstern S, Richter A.** 2012. Influence of litter chemistry and stoichiometry on glucan depolymerization during decomposition of beech (*Fagus sylvatica* L.) litter. Soil Biol Biochem **50:**174-187.

70. **Geisseler D, Horwath WR.** 2009. Relationship between carbon and nitrogen availability and extracellular enzyme activities in soil. Pedobiologia **53:**87-98.

71. **Goodfellow M.** 2012. Phylum XXVI. Actinobacteria phyl. nov. *In* Goodfellow M, Kampfer P, Busse H, Trujillo ME, Suzuki K, Ludwig W, Whitman WB (ed.), Bergey's manual of systematic bacteriology, vol 5. The *Actinobacteria,* part A. Springer, New York.

72. **Simpson AJ, Song G, Smith E, Lam B, Novotny EH, Hayes MHB.** 2007. Unraveling the structural components of soil humin by use of solution-state nuclear magnetic resonance spectroscopy. Environ Sci Technol **41:**876-883.

73. **Spence A, Simpson AJ, McNally DJ, Moran BW, McCaul MV, Hart K, Paull B, Kelleher BP.** 2011. The degradation characteristics of microbial biomass in soil. Geochim Cosmochim Ac **75:**2571-2581.

74. **Baldrian P, Kolařík M, Štursová M, Kopecký J, Valášková V, Větrovský T, Zifčáková L, Šnajdr J, Rídl J, Vlček C, Voříšková J.** 2012. Active and total microbial communities in forest soil are largely different and highly stratified during decomposition. ISME J **6:**248-258.

75. **Rooney DC, Clipson NJW.** 2009. Phosphate addition and plant species alters microbial community structure in acidic upland grassland soil. Microb Ecol **57:**4-13.

76. **Irving GCJ, McLaughlin MJ.** 1990. A rapid and simple field test for phosphorus in Olsen and Bray No. 1 extracts of soil. Commun Soil Sci Plan **21:**2245-2255.

77. **Olsen SR, Sommers LE.** 1982. Phosphorus. Methods of soil analysis. Part 2. Chemical and microbiological properties**:**403-430.

Tables

Table 1. PERMANOVA values for differences in GH48 gene community composition between land uses and sites. Pairwise comparisons show differences between sites within land uses and between land uses within sites. Pseudo-*F* values and *t*-statistics are shown for the main test and pairwise comparisons respectively. For PERMANOVA there were 2 factors: site [3 levels (Talmo, Glenrock and Bogo)], and land use [2 levels (woodland and pasture)].

Test	Factor	Pairwise comparisons	Pseudo-*F*	*t* statistic	*P*-value
Main test	Land use		30.886		< 0.001
	Site		11.785		< 0.001
	Site vs. Land-use interaction		10.29		< 0.001
Pairwise - Woodland	Site	TO versus GK		2.782	< 0.001
Pairwise - Woodland	Site	TO versus BO		3.709	< 0.001
Pairwise - Woodland	Site	GK versus BO		2.210	< 0.001
Pairwise - Pasture	Site	TO versus GK		4.316	< 0.001
Pairwise Pasture	Site	TO versus BO		3.724	< 0.001
Pairwise Pasture	Site	GK versus BO		3.313	< 0.001
Pairwise - TO	Land use	Pasture versus woodland		5.171	< 0.001
Pairwise - GK	Land use	Pasture versus woodland		2.993	< 0.001
Pairwise BO	Land use	Pasture versus woodland		4.352	< 0.001

Table 2. Global multivariate dispersion analysis (MVDISP) for GH48, fungal ITS genes and bacterial 16S rRNA for each land use and SIMPER analysis of soil variables (contribution of variables to similarity). Shared superscripts within MVDISP columns for individual plot tests indicate significant differences in homogeneity of dispersion between two specific plots (PERMDISP).

Test	Factor	MVDISP Dispersion			SIMPER averaged squared distance
		GH48	Fungi	Bacteria	Environmental variables
Land use test	Woodland	1.186*	1.323^{+}	0.999	23.76
	Pasture	0.807*	0.677^{+}	1.001	13.87
Individual plot test	TW	1.214^{ab}	1.384^{abcd}	1.368^{abcd}	19.45
	GW	1.314^{f}	1.286^{ehij}	0.816^{bf}	22.75
	BW	1.124^{ch}	1.561^{cfikm}	1.345^{efgh}	31.20
	TP	0.456^{acde}	0.514^{aefg}	0.809^{ae}	13.68
	GP	1.232^{dg}	0.456^{bhkl}	0.78^{cg}	15.07
	BP	$0.622b^{efgh}$	0.778^{dgjlm}	0.855^{dh}	18.00

TW, Talmo woodland; GW, Glenrock woodland; BW, Bogo woodland; TP, Talmo pasture; GP, Glenrock pasture; BP, Bogo pasture.

Table 3. DistLM models showing variables that best explain variation in GH48, bacterial 16S rRNA and fungal ITS community composition. Variables are ordered based on decreasing percentage contribution to total explained variability (in parentheses). R^2 values indicate the overall amount of variability explained by the model. Abbreviations for soil variables are as indicated in the methods; HOC is in bold to highlight its importance for the different groups.

Land use	**Microbial community**	**Factors (*P* value < 0.05) % contribution of each variable in brackets**	**R^2**
Woodland + Pasture	**GH48**	C:N ratio (9.06), soil moisture (5.51), pH (2.31), clay (2.30), **HOC (2.00)**, POC (1.50), MBC (1.41), DON (0.98), Inorg P (0.83), ROC (0.73), MBN (0.64), NH_4^+-N (0.57)	0.23
	Bacteria	C:N ratio (7.84), Org P (5.67), MBC (5.13), soil moisture (3.79), pH (2.81), clay (2.50), Inorg P (1.44), ROC (1.27), POC (0.92), DOC (0.88), DON (0.86), **HOC (0.69)**, NH_4^+-N (0.59), FAA-N (0.57)	0.35
	Fungi	C:N ratio (9.29), soil moisture (3.85), pH (2.06), Inorg P (1.72), clay (1.38), POC (1.14), **HOC (1.02)**, ROC (0.86), Org P (0.65), FAA-N (0.63) MBC (0.59), DON (0.57), NH_4^+-N (0.53), NO_3^--N (0.47)	0.25
Woodland	**GH48**	C:N ratio (5.47), pH (5.44), **HOC (2.21)**, soil moisture (2.08), FAA-N (1.49)	0.16
	Bacteria	pH (10.65), C:N ratio (5.86), NH_4^+-N (3.72), MBC (1.96), DOC (1.96), DON (1.86), clay (1.59), MBN (1.40), LOI (1.36), Inorg P (1.32), FAA-N (1.15), ROC (1.13), NO_3^--N (1.02), **HOC (0.99)**	0.36
	Fungi	pH (3.51), C:N ratio (2.57), LOI (1.80), MBC (1.26), ROC (1.14), POC (1.05), FAA-N (1.05)	0.13
Pasture	**GH48**	Soil moisture (11.95), **HOC (4.44)**, clay (2.31), POC (1.71), pH (1.23)	0.21
	Bacteria	Inorg P (16.09), soil moisture (11.80), MBN (5.51), clay (3.40), pH (3.06), ROC (2.12), **HOC (2.05)**, POC (1.19), DON (1.40)	0.47
	Fungi	Soil moisture (13.81), Inorg P (5.28), clay (1.81), pH (1.65), MBN (1.31), Org P (1.29), **HOC (1.17)**, POC (1.14), ROC (0.97) C:N ratio (0.96)	0.29

Figures

Figure 1. Maximum likelihood tree (RaxML) constructed with GH48 sequences from soil clones and cultured strains from Actinobacteria, Firmicutes, Neocallimastigales (anaerobic fungi), Proteobacteria, Chloroflexi and Insecta. Nodes in tree branches indicate bootstrap support > 0.8. Sequences from *Bacillus* spp. and *Paenibacillus* spp. were used as outgroups. Sequence accessions are indicated following strain name. Colours indicate sequence taxonomy or soil clone provenance; symbols in front of sequence names indicate the presence or absence of aromatic amino acids relevant to cellulolytic action in *T. fusca.* Filled black circles indicate the presence of both amino acids, filled grey circles indicate lack of phenylalanine 195, diamonds indicate lack of tyrosine 213, open circles indicate the lack of both aromatic amino acids. TW, Talmo woodland; GW, Glenrock woodland; BW, Bogo woodland; TP, Talmo pasture; GP, Glenrock pasture; BP, Bogo pasture.

Figure 2. Principal coordinate (PCO) analysis of GH48 (A), bacterial (B) and fungal (C) community composition for all sites and land uses generated by T-RFLP. Colours indicate sites, triangles represent woodland samples, circles represent pasture samples. Vectors included were those that had a length > 0.4. The large circle is a unit circle with radius = 1.

Figure 3. Total abundance per gram of soil of actinobacterial GH48, bacterial 16S rRNA and fungal ITS genes. Error bars are standard errors. TW, Talmo woodland; GW, Glenrock woodland; BW, Bogo woodland; TP, Talmo pasture; GP, Glenrock pasture; BP, Bogo pasture.

Figure 1

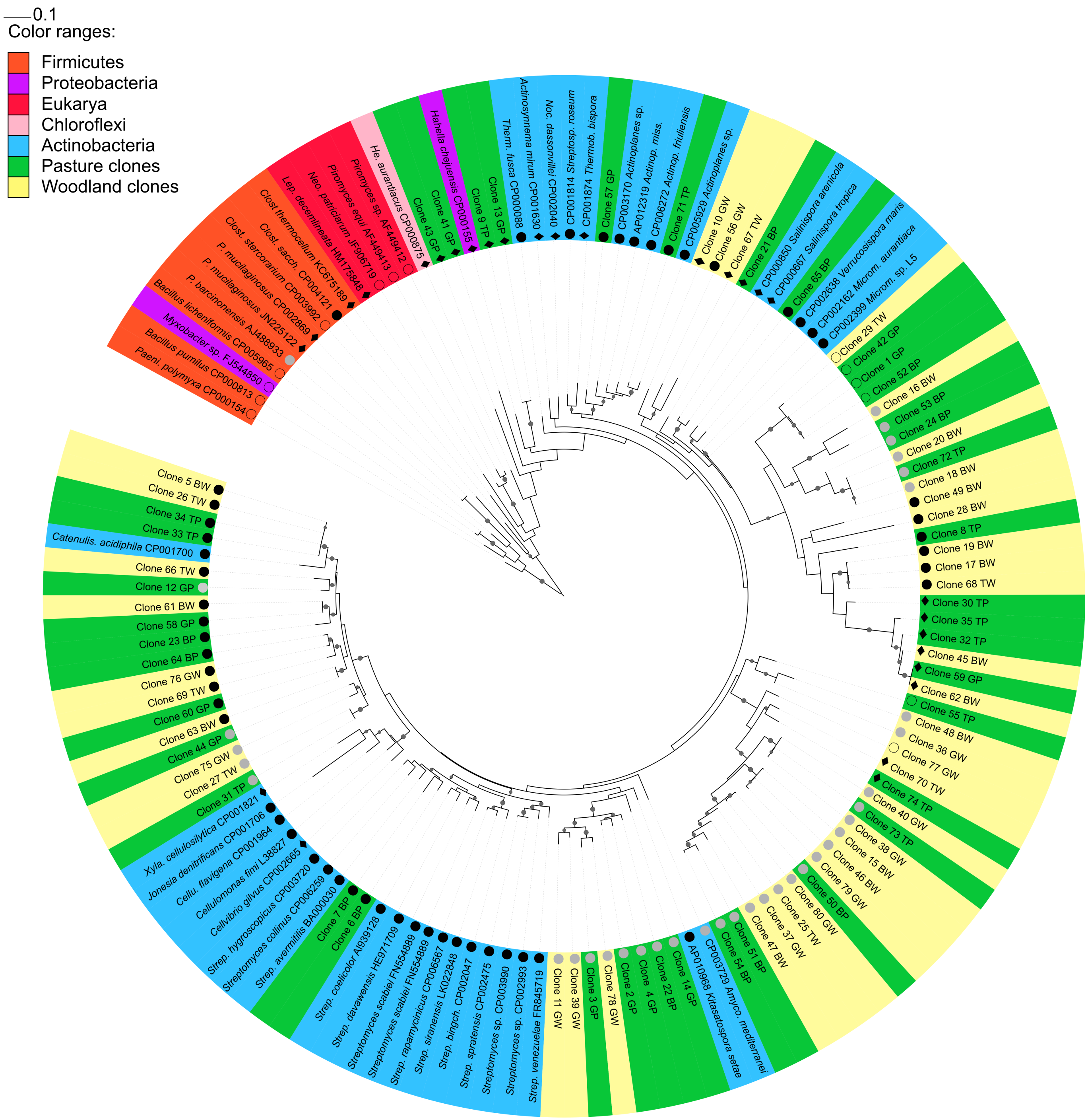
0.1
Color ranges:
Firmicutes
Proteobacteria
Eukarya
Chloroflexi
Actinobacteria
Pasture clones
Woodland clones
Paeni. polymyxa CP000154
Bacillus pumilus CP000813
Myxobacter sp. FJ544850
Bacillus licheniformis CP005965
P. barcinonensis AJ488933
P. mucilaginosus JN225122
P. mucilaginosus CP002869
Clost. stercorarium CP003992
Clost. sacch. CP004121
Clost thermocellum KC675189
Lep. decemlineata HM175848
Neo. patriciarum JF906719
Piromyces equi AF449413
Piromyces sp. AF449412
He. aurantiacus CP000875
Clone 43 GP
Clone 41 GP
Hahella chejuensis CP000155
Clone 9 TP
Clone 13 GP
Therm. fusca CP000088
Actinosynnema mirum CP001630
Noc. dassonvillei CP002040
CP001814 Streptosp. roseum
CP001874 Thermob. bispora
Clone 57 GP
CP003170 Actinoplanes sp.
AP012319 Actinop. miss.
CP006272 Actinop. friuliensis
Clone 71 TP
CP005929 Actinoplanes sp.
Clone 10 GW
Clone 56 GW
Clone 67 TW
Clone 21 BP
CP000850 Salinispora arenicola
CP000667 Salinispora tropica
Clone 65 BP
CP002638 Verrucosispora maris
CP002162 Microm. aurantiaca
CP002399 Microm. sp. L5
Clone 29 TW
Clone 42 GP
Clone 1 GP
Clone 52 BP
Clone 16 BW
Clone 53 BP
Clone 24 BP
Clone 20 BW
Clone 72 TP
Clone 18 BW
Clone 49 BW
Clone 28 BW
Clone 8 TP
Clone 19 BW
Clone 17 BW
Clone 68 TW
Clone 30 TP
Clone 35 TP
Clone 32 TP
Clone 45 BW
Clone 59 GP
Clone 62 BW
Clone 55 TP
Clone 48 BW
Clone 36 GW
Clone 77 GW
Clone 70 TW
Clone 74 TP
Clone 40 GW
Clone 73 TP
Clone 38 GW
Clone 15 BW
Clone 46 BW
Clone 79 GW
Clone 50 BP
Clone 80 GW
Clone 25 TW
Clone 37 GW
Clone 47 BW
Clone 51 BP
Clone 54 BP
CP003729 Amyco. mediterranei
AP010968 Kitasatospora setae
Clone 14 GP
Clone 22 BP
Clone 4 GP
Clone 2 GP
Clone 78 GW
Clone 3 GP
Clone 39 GW
Clone 11 GW
Strep. venezuelae FR845719
Streptomyces sp. CP002993
Streptomyces sp. CP003990
Strep. spratensis CP002475
Strep. bingch. CP002047
Strep. siranensis LK022848
Strep. rapamycinicus CP006567
Streptomyces scabiei FN554889
Strep. davawensis HE971709
Strep. coelicolor AI939128
Clone 6 BP
Clone 7 BP
Strep. avermitilis BA000030
Streptomyces collinus CP006259
Strep. hygroscopicus CP003720
Cellvibrio gilvus CP002665
Cellulomonas fimi L38827
Cellu. flavigena CP001964
Jonesia denitrificans CP001706
Xyla. cellulosilytica CP001821
Clone 31 TP
Clone 27 TW
Clone 75 GW
Clone 44 GP
Clone 63 BW
Clone 60 GP
Clone 69 TW
Clone 76 GW
Clone 64 BP
Clone 23 BP
Clone 58 GP
Clone 61 BW
Clone 12 GP
Clone 66 TW
Catenulis. acidiphila CP001700
Clone 33 TP
Clone 34 TP
Clone 26 TW
Clone 5 BW

Figure 2

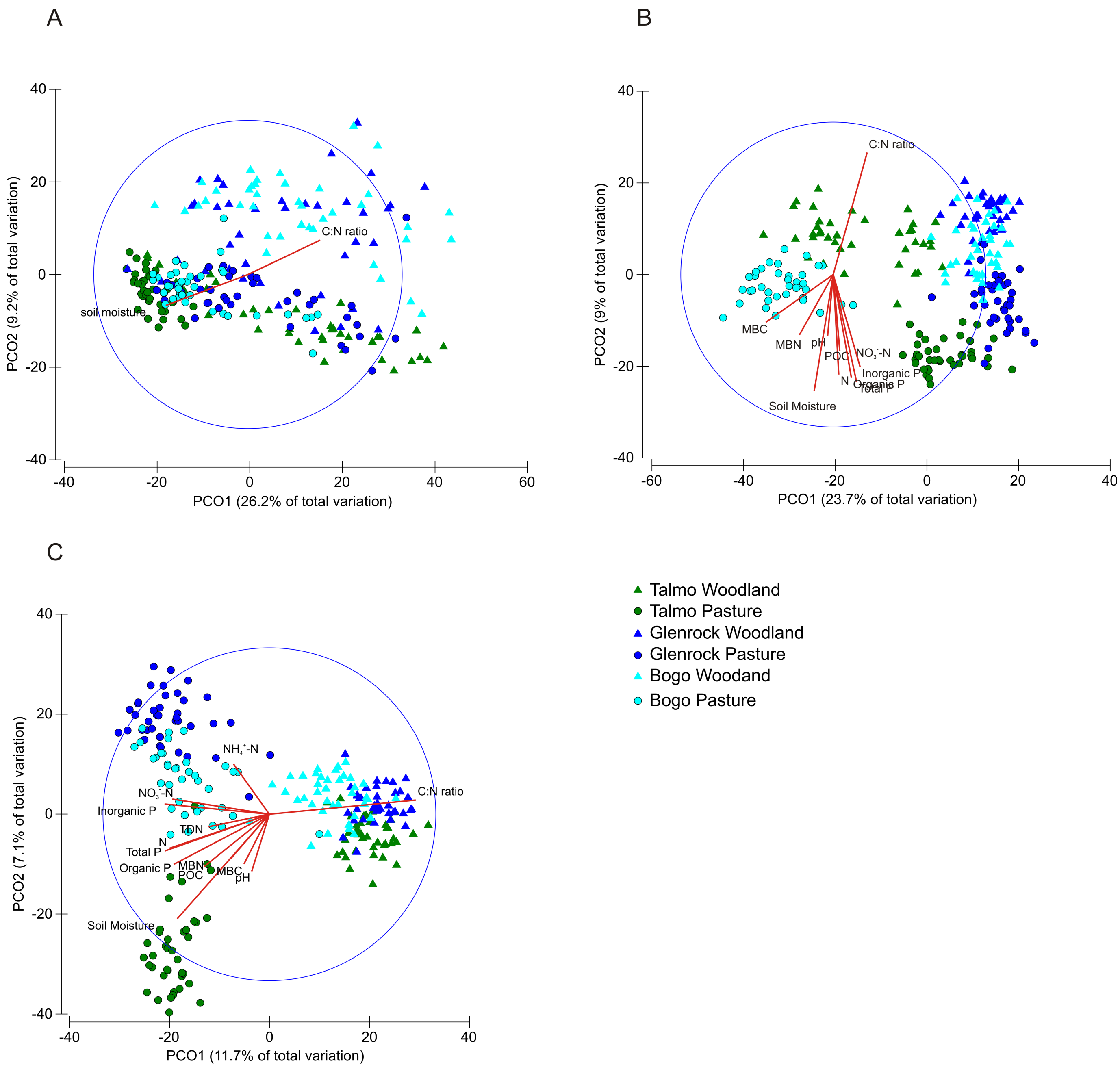
A
PCO2 (9.2% of total variation)
PCO1 (26.2% of total variation)
C:N ratio
soil moisture
B
PCO2 (9% of total variation)
PCO1 (23.7% of total variation)
C:N ratio
MBC
MBN
pH
POC
NO3-N
Inorganic P
N
Organic P
Total P
Soil Moisture
C
PCO2 (7.1% of total variation)
PCO1 (11.7% of total variation)
NH4+-N
NO3-N
Inorganic P
C:N ratio
TDN
N
Total P
Organic P
MBN
POC
MBC
pH
Soil Moisture
Talmo Woodland
Talmo Pasture
Glenrock Woodland
Glenrock Pasture
Bogo Woodand
Bogo Pasture

Figure 3

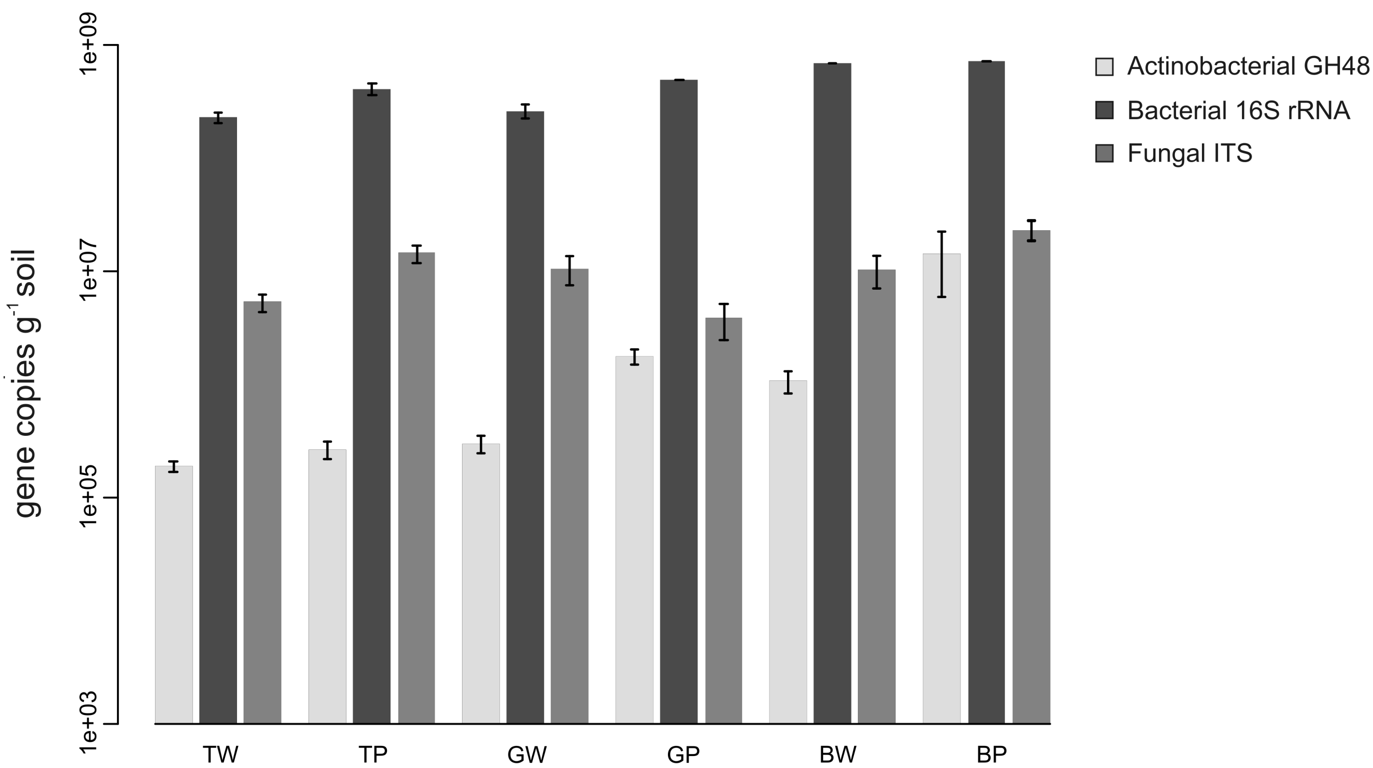
gene copies g^{-1} soil
1e+09
1e+07
1e+05
1e+03
TW
TP
GW
GP
BW
BP
Actinobacterial GH48
Bacterial 16S rRNA
Fungal ITS